

## Molecular monolayers for conformal, nanoscale doping of InP nanopillar photovoltaics

Kee Cho, Daniel J. Ruebusch, Min Hyung Lee, Jae Hyun Moon, Alexandra C. Ford, Rehan Kapadia, Kuniharu Takei, Onur Ergen, and Ali Javey<sup>a)</sup>

Electrical Engineering and Computer Science, University of California, Berkeley, California 94720, USA and Materials Sciences Division, Lawrence Berkeley National Laboratory, Berkeley, California 94720, USA and Berkeley Sensor and Actuator Center, University of California, Berkeley, California 94720, USA

(Received 23 March 2011; accepted 12 April 2011; published online 17 May 2011)

Semiconductor nanopillar arrays with radially doped junctions have been widely proposed as an attractive device architecture for cost effective and high efficiency solar cells. A challenge in the fabrication of three-dimensional nanopillar devices is the need for highly abrupt and conformal junctions along the radial axes. Here, a sulfur monolayer doping scheme is implemented to achieve conformal ultrashallow junctions with sub-10 nm depths and a high electrically active dopant concentration of  $10^{19}$ – $10^{20}$  cm<sup>-3</sup> in arrays of InP nanopillars. The enabled solar cells exhibit a respectable conversion efficiency of 8.1% and a short circuit current density of 25 mA/cm<sup>2</sup>. The work demonstrates the utility of well-established surface chemistry for fabrication of nonplanar junctions for complex devices. © 2011 American Institute of Physics. [doi:10.1063/1.3585138]

Recent advancements in the large-scale fabrication of three-dimensional (3D) nanopillar (NPL) arrays have attracted tremendous research in their utilization for various electronics, sensing, and energy applications.<sup>1–4</sup> Specifically, NPLs provide advantages over conventional thin films in terms of photon management and carrier collection efficiency for photovoltaic (PV) devices. For NPL cells, the dominant carrier loss mechanism is surface recombination due to the high surface area to volume ratio.<sup>5</sup> The surface recombination velocities of untreated CdS,<sup>6</sup> CdTe,<sup>7</sup> CIGS,<sup>8</sup> and InP (Ref. 9) have been reported to be  $10^2$ – $10^4$  cm s<sup>-1</sup>. The low surface recombination rates of these material systems, without complex surface treatment, make them ideal candidates for high efficiency NPL cells. In this regard, here we focus on the use of InP NPLs with radial *p-n* junctions for PV applications.

A challenge in designing NPL PV devices is the requirement to form ultrashallow (sub-10 nm) and conformal *p-n* junctions along the radial orientation. This can be achieved *in situ* by controlling the catalytic growth versus surface coating rates.<sup>3</sup> *Ex situ* doping may be more attractive due to process simplicity and better control of the device architecture. The conventional methods for semiconductor doping fall short when trying to fabricate 3D junctions with controlled dimensions. For instance, gas phase doping techniques lack the desired control in the dopant areal dose and surface coverage uniformity. Ion implantation does not provide conformal dopant incorporation for 3D structures and, induces significant lattice damage that could significantly enhance the minority carrier recombination rates. In this letter, we report a versatile and generic approach of surface doping InP NPL arrays by the use of sulfur self-assembled monolayers (SAMs). This molecular monolayer doping (MLD) approach<sup>10–12</sup> enables the ultrashallow incorporation of dopants at high concentrations in the surface of NPLs, resulting in high quality, radial (i.e., core/shell) *p-n* junctions. Given the self-limiting nature of SAMs, a highly uniform surface

coverage of S atoms is obtained on the exposed InP surfaces which provides excellent control over the incorporated dopant dose during the subsequent thermal annealing step.

The fabrication process of the InP NPL solar cell is shown in Fig. 1. *p*-InP (100) wafers, doped with Zn at a concentration of  $\sim 2 \times 10^{17}$  cm<sup>-3</sup>, were used as the starting substrates. First, 30 nm of Cr was deposited using electron-beam evaporation on the backside of the wafer to protect the back surface from subsequent processing steps. The top surface of InP was cleaned with O<sub>2</sub> plasma to remove organic contaminants. Monodispersed 540 nm silica beads were spin-coated at 1100 rpm (ramp-up rate of 100 rpm/min) on the front side of the substrate. Figure 2(a) shows a scanning electron microscope (SEM) image of spin-coated silica beads, exhibiting uniform monolayer coverage with hexagonal packing. Using silica beads as a mask, InP was etched by

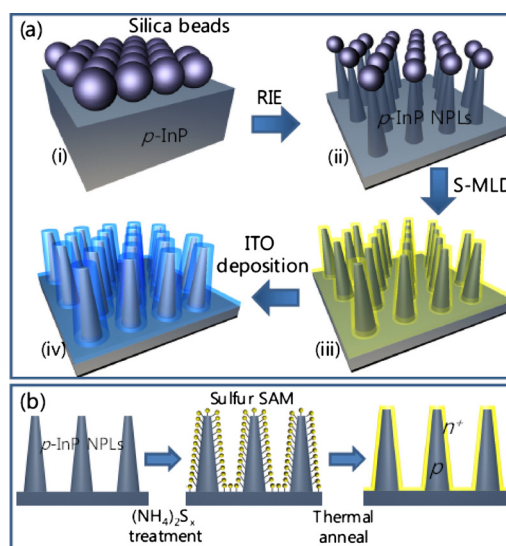


FIG. 1. (Color online) (a) The fabrication process schematic of InP NPL solar cells, involving (i) silica beads (diameter of  $\sim 540$  nm) assembly on a bulk *p*-InP wafer, (ii) InP RIE and silica beads wet etching, (iii) S-MLD of NPLs, and (iv) sputtering of ITO top contact. (b) Detailed process schematic of the S-MLD process.

<sup>a)</sup>Electronic mail: ajavey@berkeley.edu.

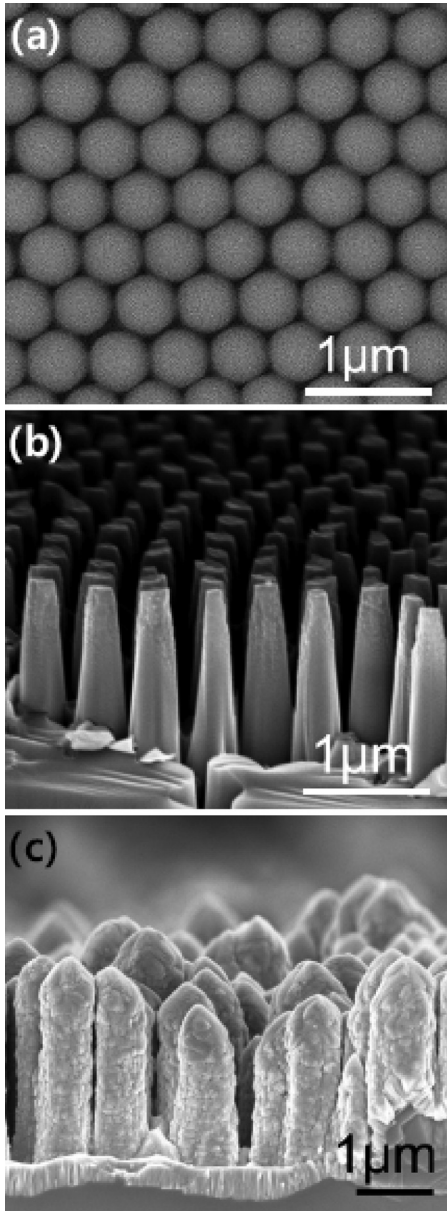


FIG. 2. SEM images of (a) spin-coated silica beads, (b) as-made NPLs, and (c) NPLs coated with ITO ( $\sim 100$  nm thick).

a two-step reactive-ion etching (RIE): (1) shrinking of silica beads using 100 SCCM (SCCM denotes cubic centimeter per minute at STP)  $\text{CHF}_3$  and 4 SCCM  $\text{O}_2$  at 50 W for 3 min; (2) dry etching of InP using 10 SCCM  $\text{CH}_4$ , 80 SCCM  $\text{H}_2$ , and 10 SCCM Ar at 200 W rf power for 90 min. After RIE, silica beads were removed in 2% HF and the surface of the NPLs were cleaned by dipping in 1% HCl and 1%  $\text{HNO}_3$  solutions for 1 min each. During this step, the physically damaged and nonstoichiometric oxidized surface layers were removed. The SEM image of the fabricated NPL arrays is shown in Fig. 2(b). The pitch between the pillars is approximately 400 nm. This subwavelength pattern reduces the reflectance from 30% (bare InP wafer) to less than 5% for a wavelength range of 450–800 nm.

Conformal surface n-doping of InP NPLs was achieved by the use of the MLD technique [Fig. 1(b)]. MLD has been shown in the past to successfully dope planar Si (Refs. 10 and 11) and InAs (Ref. 12) planar substrates with extremely low junction depths down to 2–3 nm. Here, we extend this process to nonplanar, NPL substrates, taking advantage of

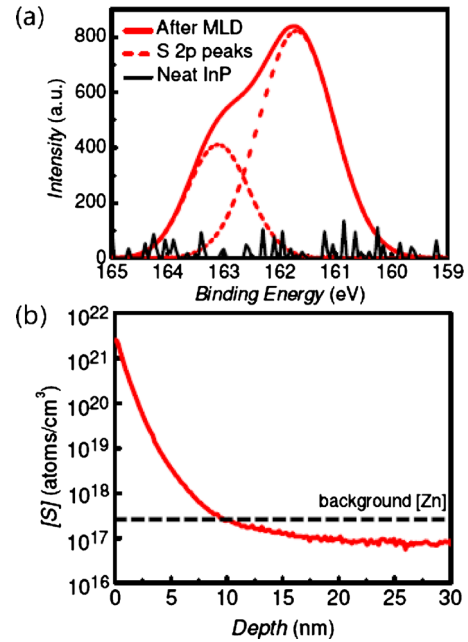


FIG. 3. (Color online) (a) XPS surface characterization of a planar *p*-InP wafer after supersaturated ammonium sulfide treatment. (b) Sulfur SIMS profile of an InP wafer after the S-MLD process. The dashed line shows the background Zn concentration of  $2 \times 10^{17}$  cm<sup>-3</sup>.

the conformal monolayer coverage on 3D structures. A SAM of S was first formed on the InP NPL surfaces using the well-established solution chemistry introduced previously.<sup>13,14</sup> Briefly, 15 ml of ammonium sulfide (20% in DI water) was prepared and placed in a 35 °C water bath. In order to supersaturate the ammonium sulfide solution with sulfur, 0.2 g of sulfur was added. The InP NPL sample was placed in the solution for 15 min then rinsed thoroughly with DI water. A 100 nm  $\text{SiO}_x$  film was deposited by electron-beam evaporation onto the surface as a capping layer. Sulfur was then thermally diffused into *p*-InP NPLs using a tube furnace at 570 °C and 650 torr under a  $\text{N}_2$  ambient for 15 min. During the thermal diffusion process, it is critical to have a high partial vapor pressure of phosphorus to prevent surface desorption of phosphorus atoms from the substrate, which could lead to the formation of an indium rich surface layer. Thus,  $\sim 100$  mg of red phosphorus was placed near the sample during the thermal annealing step.

Following the S-MLD process, a bilayer of Zn/Au was deposited on the back surface and annealed at 400 °C. During this step, Zn diffuses into the back side creating a  $p^+$  layer and enabling an Ohmic back contact to *p*-InP substrate.<sup>15</sup> Next, the  $\text{SiO}_x$  capping layer was removed from the top surface in 1% HF and  $\sim 100$  nm of indium tin oxide (ITO) was sputtered as the top contact. ITO was annealed using rapid thermal annealing at 350 °C in a  $\text{N}_2$  ambient. Figure 2(c) shows the SEM image of a fully fabricated InP NPL cell.

The S monolayer formation on InP surface after ammonium sulfide treatment was characterized by x-ray photoelectron spectroscopy (XPS) in an ultrahigh vacuum chamber ( $10^{-9}$  torr) at room temperature with a monochromated Al  $K\alpha$  source and pass energy set to 35.75 eV. Figure 3(a) shows the S 2*p* peak spectra for a monolayer-reacted InP substrate with S 2*p*<sub>3/2</sub> and S 2*p*<sub>1/2</sub> doublet peak fits. A peak at  $\sim 162$  eV is observed, which is the binding energy of core shell electrons for the sulfur 2*p* shell.<sup>13,14</sup>

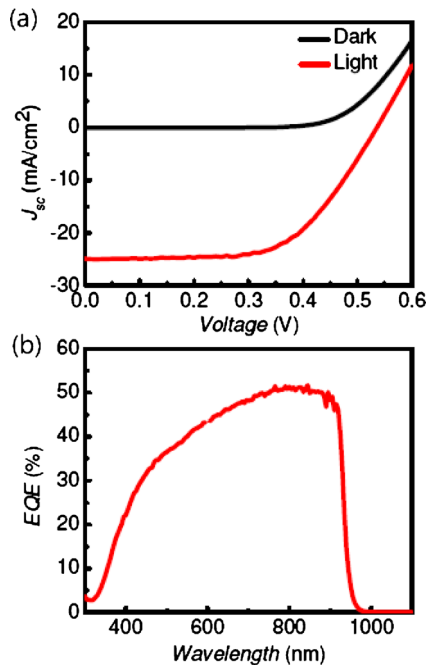


FIG. 4. (Color online) Characterization of InP NPL solar cells. (a)  $I$ - $V$  characteristics under dark and AM 1.5G illumination. (b) EQE as a function of wavelength.

Secondary-ion mass spectrometry (SIMS) was used to characterize the S dopant profile obtained by the MLD process. Figure 3(b) shows the SIMS profile of a planar InP substrate after S-MLD. A high S surface concentration [ $S$ ]  $> 10^{21}$   $\text{cm}^{-3}$  is observed which rapidly decays at an inverse slope of  $\sim 1.25$  nm/dec for the first  $\sim 4$  nm. Given a background Zn concentration of  $\sim 2 \times 10^{17}$   $\text{cm}^{-3}$ , an ultrashallow junction depth of  $\sim 10$  nm is obtained from the SIMS profile. From the published diffusion coefficient of sulfur in InP,  $D_S \sim 9 \times 10^{-16}$   $\text{cm}^2/\text{s}$ ,<sup>16</sup> and the diffusion time,  $t = 15$  min, a characteristic diffusion length of  $(D_S t)^{1/2} \sim 9$  nm is predicted, which correlates well with the SIMS data. From Hall effect measurements, the concentration of electrically active S dopants was determined to be  $10^{19}$ – $10^{20}$  atoms/ $\text{cm}^3$ , assuming a junction depth of 10 nm.

The current-voltage,  $I$ - $V$ , characteristics of the InP NPL cells were measured at room temperature using a simulated AM 1.5 global spectrum [Fig. 4(a)]. An efficiency of  $\sim 8.1\%$  is obtained with an open circuit voltage  $V_{oc} = 0.54$  V, short circuit density  $J_{sc} = 25$   $\text{mA cm}^{-2}$  and fill factor (FF)  $\sim 60\%$ . The total cell area was  $0.3 \times 0.3$   $\text{cm}^2$ . The state-of-art crystalline InP homojunction solar cell has an efficiency of  $\sim 22.1\%$ ,  $V_{oc} \sim 0.88$  V,  $J_{sc} \sim 29.5$   $\text{mA cm}^{-2}$ , and FF  $\sim 85.4\%$ .<sup>17</sup> The performance of our device is limited by the quality of top and bottom contacts, absence of an antireflective coating, and the quality of the NPL surfaces. From Fig. 4(a), a high series resistance is evident while the parallel shunt resistance is minimal. For planar InP solar cells which were doped through a similar S-MLD method (results not shown), an open circuit voltage  $V_{oc} \sim 0.7$  V was achieved. The  $\sim 0.16$  V difference in  $V_{oc}$  between NPL and planar samples may arise from the surface damage of NPLs during the RIE process. The absolute external quantum efficiency (EQE) of the cell was obtained by using a Xe light

source attached to a monochromator with a resolution of 5nm and a calibrated Si reference cell [Fig. 4(b)]. A peak EQE of  $\sim 50\%$  is obtained at a wavelength of  $\sim 800$  nm. Although respectable, the results suggest that the RIE-processed NPLs exhibit a high surface recombination loss, and require further material optimization for efficiency enhancement.

In summary, InP NPL solar cells with highly abrupt and heavily doped emitter layers were fabricated by using a S-MLD scheme. Given the self-limiting nature of S monolayers on InP surfaces, a conformal doping of NPLs along the radial direction is enabled. This presents a viable route toward controlled dopant profiling of 3D semiconductors based on their well-established surface chemistries. Importantly, MLD is an equilibrium based process that does not induce lattice damage during dopant incorporation, which is in distinct contrast to ion implantation. Although wet chemistry was used here for sulfur SAM formation, in the future, gas-based MLD processes, for instance by using hydrogen sulfide as the monolayer precursor, can be explored to further enhance the manufacturability of this process technology.

This work was supported by Mohr Davidow Ventures and NSF (Grant No. 0826145). The S-MLD process development was supported by a LDRD from LBNL. A.J. acknowledges a Sloan research fellowship and support from the World Class University program at Sunchon National University. J.M. acknowledges financial support from Korea Institute for Advancement of Technology (KIAT). R.K. acknowledges an NSF Graduate Fellowship.

- <sup>1</sup>Z. Fan, H. Razavi, J.-W. Do, A. Moriwaki, O. Ergen, Y.-L. Chueh, P. W. Leu, J. C. Ho, T. Takahashi, L. A. Reichertz, S. Neale, K. Yu, M. Wu, J. W. Ager, and A. Javey, *Nature Mater.* **8**, 648 (2009).
- <sup>2</sup>M. D. Kelzenberg, S. W. Boettcher, J. A. Petykiewicz, D. B. Turner-Evans, M. C. Putnam, E. L. Warren, J. M. Spurgeon, R. M. Briggs, N. S. Lewis, and H. A. Atwater, *Nature Mater.* **9**, 239 (2010).
- <sup>3</sup>B. Tian, X. Zheng, T. J. Kempa, Y. Fang, N. Yu, G. Yu, J. Huang, and C. M. Lieber, *Nature (London)* **449**, 885 (2007).
- <sup>4</sup>Z. Fan, D. J. Ruebusch, A. A. Rathore, R. Kapadia, O. Ergen, P. W. Leu, and A. Javey, *Nano Res.* **2**, 829 (2009).
- <sup>5</sup>R. Kapadia, Z. Fan, and A. Javey, *Appl. Phys. Lett.* **96**, 103116 (2010).
- <sup>6</sup>Y. Rosenwaks, L. Burstein, Y. Shapira, and D. Huppert, *Appl. Phys. Lett.* **57**, 458 (1990).
- <sup>7</sup>R. Cohen, V. Lyahovitskaya, E. Poles, A. Liu, and Y. Rosenwaks, *Appl. Phys. Lett.* **73**, 1400 (1998).
- <sup>8</sup>W. K. Metzger, I. L. Repins, M. Romero, P. Dippo, M. Contreras, R. Noufi, and D. Levi, *Thin Solid Films* **517**, 2360 (2009).
- <sup>9</sup>C. A. Hoffman, K. Jarasunas, H. J. Gerritsen, and A. V. Nurmikko, *Appl. Phys. Lett.* **33**, 536 (1978).
- <sup>10</sup>J. C. Ho, R. Yerushalmi, Z. A. Jacobson, Z. Fan, R. L. Alley, and A. Javey, *Nature Mater.* **7**, 62 (2008).
- <sup>11</sup>J. C. Ho, R. Yerushalmi, G. Smith, P. Majhi, J. Bennett, J. Halim, V. N. Faifer, and A. Javey, *Nano Lett.* **9**, 725 (2009).
- <sup>12</sup>J. C. Ho, A. C. Ford, Y.-L. Chueh, P. W. Leu, O. Ergen, K. Takei, G. Smith, P. Majhi, J. Bennett, and A. Javey, *Appl. Phys. Lett.* **95**, 072108 (2009).
- <sup>13</sup>H. Oigawa, J.-F. Fan, Y. Nannichi, H. Sugahara, and M. Oshima, *Jpn. J. Appl. Phys., Part 2* **30**, L322 (1991).
- <sup>14</sup>I. K. Han, E. K. Kim, J. I. Lee, S. H. Kim, K. N. Kang, Y. Kim, H. Lim, and H. L. Park, *J. Appl. Phys.* **81**, 6986 (1997).
- <sup>15</sup>E. Kuphal, *Solid-State Electron.* **24**, 69 (1981).
- <sup>16</sup>K. K. Parat and S. K. Ghandhi, *Solid-State Electron.* **31**, 1053 (1988).
- <sup>17</sup>C. J. Keavney, V. E. Haven, and S. M. Vernon, *Proceedings of the 21st IEEE Photovoltaic Specialists Conference* (IEEE, New York, 1990), p. 141.